Compact Objects and Binaries in Dense Star Clusters
Proceedings IAU Symposium No. 398, 2026
H. M. Lee, J. Hong & R. Spurzem, eds.
doi:10.1017/S1743921325104523

Intermediate mass black holes and gravitational waves from hierarchically assembling star clusters

Antti Rantala and Natalia Lahén

Max Planck Institute for Astrophysics,
Karl-Schwarzschild-Straße 1,
D-85748, Garching, Germany
emails: anttiran@mpa-garching.mpg.de, nlahen@mpa-garching.mpg.de

Abstract. Massive star clusters form through a complex hierarchical assembly. We use simulations including post-Newtonian black hole (BH) dynamics and stellar evolution to investigate the consequences of this complex assembly for the formation of intermediate mass black holes (IMBHs) by stellar collisions, tidal disruption events (TDEs) and BH mergers. At a fixed cluster mass, both the hierarchical assembly and stellar multiplicity increase the numbers (up to ~ 10 per cluster) and masses (up to $10^4 M_\odot$) of the formed IMBHs within the first 10 Myr of cluster evolution. We find that the characteristic GW fingerprint of the hierarchical star cluster assembly model is an equal-mass IMBH-IMBH merger. The IMBH masses correlate with their host star cluster properties including the cluster mass and surface density, and we predict IMBHs with masses $M_\bullet \gtrsim 10^4$ M$_\odot$ in the $z \sim 10$ star clusters recently observed by the James Webb Space Telescope.

Keywords. galaxies: star clusters: general, stars: binaries: general, stars: black holes, gravitational waves

1. Introduction

The origin of supermassive black holes (SMBHs; $M_\bullet \gtrsim 10^6$ M$_\odot$) remains a major unsolved question in modern astrophysics (Rees 1984). Observations of active galactic nuclei (AGN) indicate that accreting SMBHs with masses beyond $M_\bullet \gtrsim 10^9$ M$_\odot$ were already present at redshifts of $z \sim 6$–7 (Inayoshi *et al.* 2020) when the Universe was only a billion years old. Recent observations of AGN at redshifts up to $z \sim$ 10-11 by the James Webb Space Telescope (JWST) have only deepened the SMBH origin puzzle (Maiolino *et al.* 2024b,a; Übler *et al.* 2024). Simple Eddington rate arguments place the formation redshift of these black holes (BHs) between $z \sim 25$–20 for intermediate mass seeds ($M_\bullet \sim 10^3$–10^4 M$_\odot$) and $z \sim 15$–12 for heavy seeds ($M_\bullet \sim 10^5$ M$_\odot$). If a fraction of such SMBH seeds fail to grow, they should be observable in the local Universe (Mezcua 2017; Greene *et al.* 2020) as intermediate-mass black holes (IMBHs; 10^2 M$_\odot \lesssim M_\bullet \lesssim 10^5$ M$_\odot$).

A plausible scenario for the formation for SMBH seeds in the intermediate mass range is the stellar collisional runaway in dense star clusters (e.g. Portegies Zwart *et al.* 2004; Fregeau *et al.* 2004; Gürkan *et al.* 2004; Mapelli 2016; Arca Sedda *et al.* 2024; Rizzuto *et al.* 2021; González Prieto *et al.* 2024; Vergara *et al.* 2025b). In such a collisional cascade typically one massive star per dense star cluster can substantially grow by stellar mergers, the first collisions initiated by interactions involving initial (primordial) binary stars (Gaburov *et al.* 2008). Substantial uncertainty surrounds the evolution of

© The Author(s), 2026. Published by Cambridge University Press on behalf of The International Astronomical Union. This is an Open Access article, distributed under the terms of the Creative Commons Attribution licence (https://creativecommons.org/licenses/by/4.0/), which permits unrestricted re-use, distribution and reproduction, provided the original article is properly cited.

https://doi.org/10.1017/S1743921325104523 Published online by Cambridge University Press

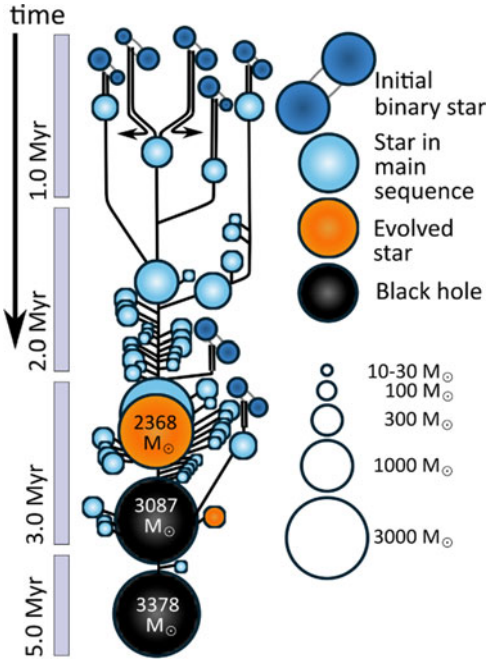


Figure 1. A stellar collisional runaway in an dense, isolated star cluster with initial binary systems. The collision cascade results in a formation of a single very massive star with a mass exceeding 3000 $M_\odot$ which collapses forming an IMBH at the end of its life (Rantala and Naab 2025).

the collision products. Strong enough stellar winds even at low metallicities may considerably affect the evolution of the collision product (e.g. Shepherd *et al.* 2025). If the wind mass loss is weak enough, the extremely massive star collapses forming an IMBH at the end of its life, otherwise no remnant is left behind (e.g. Glebbeek *et al.* 2009; Mapelli 2016). If an IMBH forms, it can grow subsequently via tidal disruption events of stars (TDEs; e.g. Rizzuto *et al.* 2023) or by merging with stellar BHs and potentially other IMBHs. An example of such a collisional runaway in an isolated star cluster is illustrated in Fig. 1. Indeed, early star clusters at $z \sim 10$ with sufficiently high (half-mass) surface densities of $\Sigma_h \gtrsim 10^5\,M_\odot$ have already been discovered (Adamo *et al.* 2024), and the observed high nitrogen abundances at low metallicities (Bunker *et al.* 2023; Topping *et al.* 2024; Isobe *et al.* 2025) may suggest the existence of dense environments in which stellar collisions can frequently occur.

A vast majority of analytic, semi-analytic, Monte Carlo and direct N-body work on the runaway collisional IMBH formation (with a notable exception of Fujii and Portegies Zwart 2013) has focused on idealized, isolated and dense star clusters. However, massive star clusters do not form monolithically in isolation. The observations by the JWST have revealed that high redshift star formation was dense, clumpy and clustered (Fujimoto *et al.* 2024; Mowla *et al.* 2024), supported by the archaeological studies of the early Milky Way (Belokurov and Kravtsov 2022). In the local Universe, young massive star clusters in the Small and Large Magellanic Clouds, the Antennae Galaxies, M51 and NGC 4449 are surrounded by complex assemblies of star clusters of similar age (Sabbi *et al.* 2007; Fahrion and De Marchi 2024; Whitmore *et al.* 2010; Bastian *et al.* 2005; Meena *et al.* 2025). These observational facts strongly suggest that massive star clusters form through a complex hierarchical assembly, which is supported by state-of-the-art solar mass resolution hydrodynamical simulations (Lahén *et al.* 2020).

https://doi.org/10.1017/S1743921325104523 Published online by Cambridge University Press

This IAU conference proceedings based on our presentation in IAU Symposium 398 in Seoul summarizes the key findings of our recent studies Rantala *et al.* (2024), Rantala and Naab (2025) and Rantala *et al.* (2025) in the FROST-CLUSTERS project that explores the IMBH formation in massive, dense and hierarchically assembling star clusters. Besides initial binary stars, we also explore scenarios involving initial triple systems as well as massive single stars beyond the typical initial mass function (IMF) cut-off of $m_\star = 150\,\mathrm{M}_\odot$. Our hierarchical post-Newtonian simulations up to $N = 2.4 \times 10^6$ individual, binary and triple stars have revealed that both the hierarchical assembly and stellar multiplicity boost the numbers and masses of the formed IMBHs. We find that the IMBH masses strongly correlate with the physical properties of their host star clusters. Moreover, we establish that the characteristic gravitational wave (GW) fingerprint of the hierarchical star cluster assembly scenario is a rapid equal mass GW merger in the IMBH mass range, potentially detectable by the next-generation GW observatories such as the Laser Interferometer Space Antenna (LISA) and the Einstein Telescope.

2. The *N*-body code BIFROST and initial conditions for hierarchical assembly models

2.1. *BIFROST*

We perform the direct N-body simulations for our FROST-CLUSTERS project using the novel GPU accelerated direct N-body simulation code BIFROST (Rantala *et al.* 2023). Unlike most direct N-body simulation codes that use the standard forth order Hermite scheme (e.g. Makino and Aarseth 1992; Spurzem 1999; Aarseth 2003), BIFROST is based on the fourth order forward symplectic integrator (e.g. Chin 1997; Dehnen and Hernandez 2017). Specifically, we use its hierarchical implementation (Rantala *et al.* 2021) that is momentum conserving and especially efficient for simulating dynamical systems with a vast dynamical range. Small scale few body interactions such as binaries, triples, fly-bys and small clusters around IMBHs are treated using a selection of secular and regularized integration techniques (Mikkola and Tanikawa 1999; Wang *et al.* 2020b; Rantala *et al.* 2020, 2023). For BHs the equations of motion are post-Newtonian up to the order PN3.5 which allows us to follow (IM)BH binary evolution from star cluster scales of ~ 1 pc down to ~ 10 Schwarzschild radii of the BHs. At BH-BH mergers the merger remnant receives a relativistic GW recoil kick (Zlochower and Lousto 2015) which may unbind the BH from its host star cluster. If a star approaches a BH within its tidal disruption radius $R_\mathrm{t} \sim (M_\bullet/m_\star)^{1/3} R_\star$, we destroy the star and the BH accretes 50% of its mass.

The BIFROST code is now also fully coupled to the fast stellar population synthesis code SEVN† (Iorio *et al.* 2023; Mapelli *et al.* 2020; Spera *et al.* 2015). The interface between the codes is described in Rantala *et al.* (2024) and Rantala *et al.* (2025). The full coupling allows us to model both single and binary stellar evolution in the hierarchical star cluster assembly simulations. Stellar collisions occur if the radii of two stars overlap, and we assign the new mass, radius and age of the collision product using SEVN. For extremely massive collision products exceeding $600\,\mathrm{M}_\odot$ in mass we use values extrapolated from lower-mass stellar models. We note that our treatment for the extremely massive collision products is still somewhat simplified, and we will improve on these models in future studies (FROST-CLUSTERS III; Rantala el al. 2025c in prep.).

2.2. *Hierarchical initial conditions with initial stellar multiplicity*

The initial star cluster masses and the structure of our massive star cluster assembly regions are motivated by the state-of-the-art solar mass resolution hydrodynamical

† SEVN, developed by M. Mapelli's DEMOBLACK team is available at https://gitlab.com/sevncodes/sevn.

https://doi.org/10.1017/S1743921325104523 Published online by Cambridge University Press

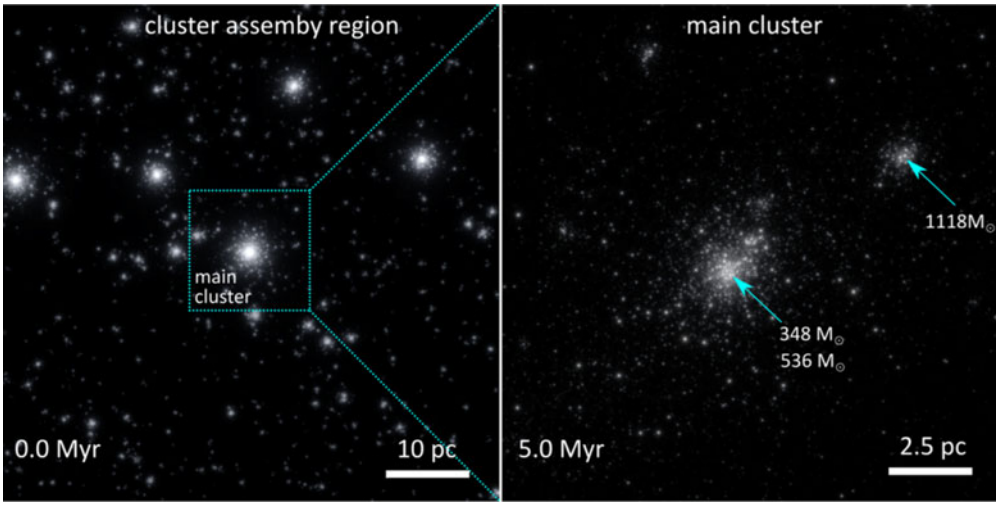


Figure 2. The rapid evolution of the hierarchical cluster assembly regions (Rantala *et al.* 2024). Left panel: the initial setup of $N = 2.4 \times 10^6$ stars in hundreds of star clusters sampled from the universal -2 power law cluster mass function. Five initial clusters are more massive just as in the $z \sim 10$ proto globular cluster observations of Adamo *et al.* (2024). Right panel: just after 5 Myr, most of the clusters are strongly interacting or have already merged and have formed IMBHs exceeding $M_\bullet \gtrsim 10^3\,\mathrm{M}_\odot$ in collisional runaways.

starburst simulations of Lahén *et al.* (2020). We sample the initial cluster masses from the universal -2 power-law cluster mass function (Elmegreen and Efremov 1996) which the hydrodynamical simulation also reproduces. We set the initial Plummer (1911) star cluster model half mass radii r_h to 1/8 of the value from Brown and Gnedin (2021) star cluster mass radius relation to capture the small sub-pc birth radii of young star clusters (Marks and Kroupa 2012). We also model the spatial extents of the cluster assembly regions (~ 50 pc) as well as the radial inflow and random velocity components (< 10 km s^{-1}) of the star cluster centre-of-masses following Lahén *et al.* (2020). We present one of our hierarchical assembly regions at $t = 0$ Myr and after approximately one dynamical time $t = 5$ Myr in Fig. 2.

For constructing the zero age main sequence stellar populations of the individual clusters we use the standard Kroupa (2001) IMF with a maximum stellar mass cut-off depending on the mass of the cluster (Yan *et al.* 2023). For massive clusters we limit the maximum initial stellar mass typically to $m_\star = 150\,\mathrm{M}_\odot$ and for a single simulation set to $m_\star = 450\,\mathrm{M}_\odot$. Note that in the high IMF cut-off case the IMF is an extended Kroupa and not top-heavy. For models with initial binaries and triples we use primary star mass dependent multiplicity fractions (Offner *et al.* 2023) with binary and triple mass ratios and orbital elements sampled using results from Moe and Di Stefano (2017) and Winters *et al.* (2019) as in the recent models of Cournoyer-Cloutier *et al.* (2021). Throughout the simulations we use a metallicity of $Z = 0.0002 = 10^{-2}\,\mathrm{Z}_\odot$.

3. Hierarchical star cluster assembly, stellar multiplicity and intermediate mass black hole formation

As shown in Fig. 2, the cluster assembly regions rapidly evolve in one dynamical time of the regions ($t_\mathrm{dyn} < 10$ Myr). The infalling star clusters strongly interact and merge with each other and most of the stellar mass ends up in the central cluster or its diffuse envelope. The individual infalling clusters have mass segregation time scales of $t_\mathrm{seg} < 1$ Myr and core collapse time scales of $0.5\,\mathrm{Myr} \lesssim t_\mathrm{cc} \lesssim 5$ Myr, so all the clusters have

https://doi.org/10.1017/S1743921325104523 Published online by Cambridge University Press

enough time to mass segregate but not necessarily core collapse during the hierarchical assembly. The core collapse timescale for all but most massive initial clusters is shorter than the life-times of most massive stars (~ 2.5 Myr) enabling runaway stellar collisions in most massive infalling sub-clusters. For the most massive sub-clusters stellar multiplicity is required to achieve a collisional runway (Rantala *et al.* 2024, 2025).

We illustrate the rich complexity of IMBH formation and IMBH-IMBH interactions in a hierarchically assembling massive star cluster with initial binary stars from Rantala and Naab (2025) in Fig. 3. Five massive sub-clusters undergo a collisional runaway initiated by single-binary and binary-binary interactions leading into the formation of one massive collision product (and thus one IMBH) per sub-cluster. Due to the rapid hierarchical star cluster assembly the IMBHs end up in the growing central massive star cluster in $\lesssim 10$ Myr, sink into its centre and initiate a phase of strong IMBH-IMBH interactions. The rich interaction phase involves both binary and triple IMBH dynamics as well as strong Newtonian and post-Newtonian interactions. Most notably, the dense cluster environment and especially the triple interactions can drive gravitational wave mergers of IMBHs both in IMBH-BH and IMBH-IMBH regime. Moreover, a rapid ($\lesssim 1.5$ Myr) phase of relatively high TDE rates up to $\Gamma \sim 5 \times 10^{-5}$ per assembling cluster follows immediately after the IMBHs have formed. At later times the IMBH TDE rates decline by 1-2 orders of magnitude.

We perform isolated comparison simulations using a reconstructed monolithic cluster with mass equal to the hierarchically formed massive cluster, starting on the zero age main sequence (Rantala *et al.* 2024). In these comparison simulations no IMBHs form. In addition, we find in all but few cases (Rantala and Naab 2025) that only a single IMBH above the pulsational pair instability mass gap can form per cluster. As the formation history (isolated vs hierarchical) of a massive star cluster determines its IMBH content, we conclude that hierarchical star cluster assembly boosts IMBH formation. Stellar multiplicity also in general increases the masses (up to 10^4 M$_\odot$) and especially the numbers of formed IMBHs (up to 10 per cluster). The most massive IMBHs in our simulations form through IMBH-IMBH mergers, suggesting a potential phase of early SMBH seed growth without accompanying electromagnetic signatures. The IMBH-IMBH mergers occasionally unbind the IMBH merger remnants due to strong GW recoil kicks. However, in our models we underestimate the escape velocity of our systems as no star cluster host galaxy potential is included. Thus, in reality, recoiling IMBHs with velocities in the range of $\sim$ a few 100 km s^{-1} would likely be retained instead of being ejected, allowing subsequent IMBH growth (Amaro-Seoane *et al.* 2014).

Tight scaling relations exist between SMBH masses and their host galaxy properties including their stellar masses and velocity dispersions (e.g. Ferrarese and Merritt 2000; Gebhardt *et al.* 2000; Häring and Rix 2004; Kormendy and Ho 2013; Reines and Volonteri 2015). We explore whether similar scaling relations exist between the formed IMBHs and their host star clusters. We focus on establishing correlations between the formed IMBH masses $M_\bullet$ and the star cluster properties such as cluster mass $M_{\rm cl}$, cluster half-mass surface density $\Sigma_{\rm h}$ and the cluster half-mass velocity dispersion σ. We present the results for the star cluster mass and half mass surface density in Fig. 4. For the case of the velocity dispersion see Rantala *et al.* (2025). In each case we find a clear correlation between $M_\bullet$ and the initial cluster properties.

We fit power-law scaling relations of the form $M_\bullet \propto M_{\rm cl}^{\alpha}$, $M_\bullet \propto \Sigma_{\rm h}^{\beta}$ and $M_\bullet \propto \sigma^{\gamma}$ to our simulation results and find $\alpha \sim 1.0$, $\beta \sim 1.5$ and $\gamma \sim 3.0$ (Rantala *et al.* 2025). The exact values for the power-law indexes depend on the initial multiplicity content of the hierarchical models. In general, models with initially only single stars show shallower power-law slopes as IMBH formation in massive high velocity dispersion single star models may be suppressed (Rantala *et al.* 2024). We note that a recent study of Vergara *et al.* (2025a) has reported a very similar scaling relation between the host cluster mass $M_{\rm cl}$ and the

https://doi.org/10.1017/S1743921325104523 Published online by Cambridge University Press

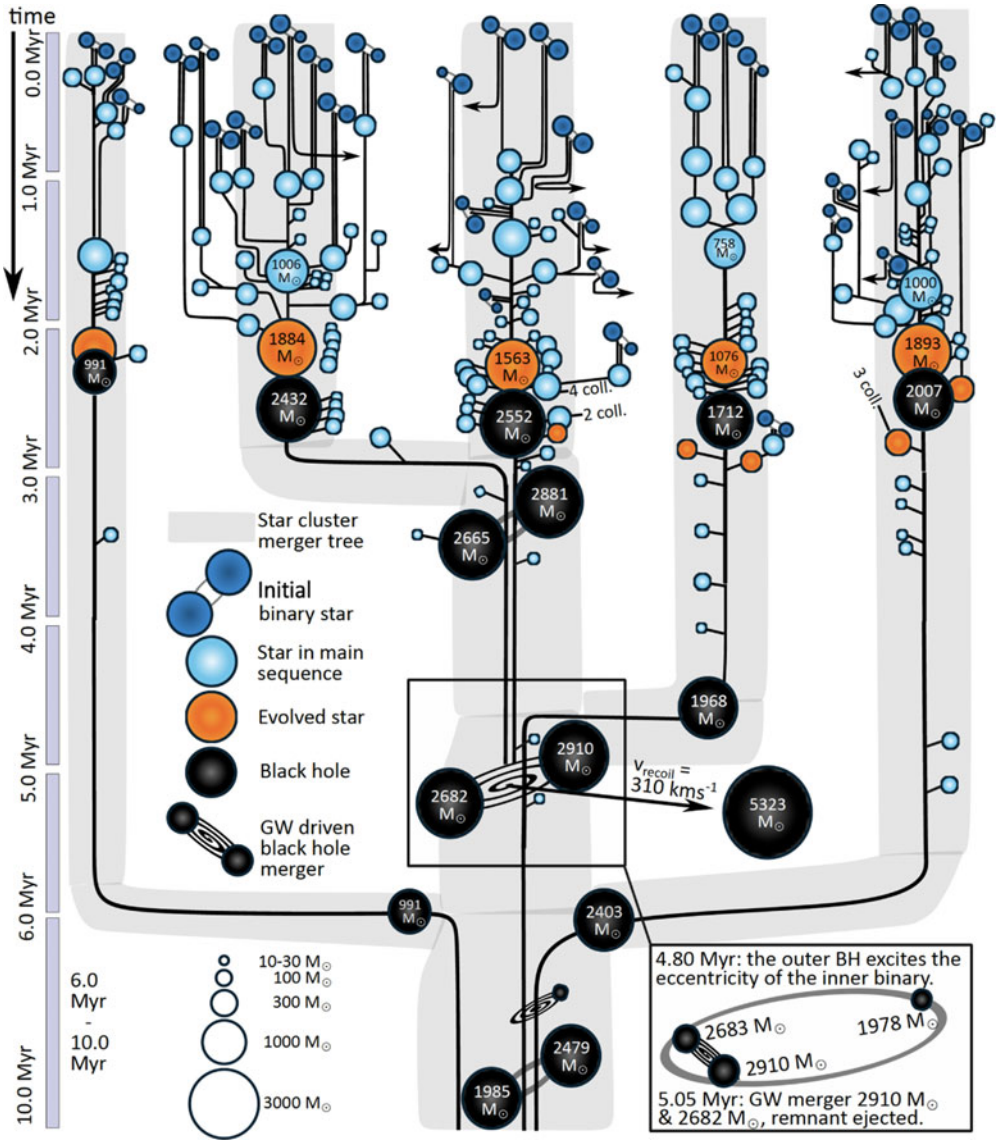


Figure 3. Multiple collisional runaways in the most massive sub-clusters of a hierarchically assembling million solar mass star cluster including initial binary stars (Rantala and Naab 2025). The contrast to the runaway collisions in the isolated star cluster of Fig. 1 is stark. In the simulation, five sub-clusters form a massive collision product that collapse into IMBHs with masses up to a few times $10^3\,\mathrm{M}_\odot$. Due to the hierarchical assembly, these IMBHs subsequently end up into the central growing star cluster and rapidly sink into its centre. A complex phase of IMBH dynamics follows including Newtonian and post-Newtonian binary and triple interactions as well as GW driven IMBH-BH and IMBH-IMBH mergers which occasionally may eject the merger remnant from the cluster via a relativistic GW recoil kick.

IMBH mass $M_\bullet$ compared to our single star model. For the velocity dispersion relation we find shallower relations compared to the galactic scale $M_\bullet$–σ relations which have $\gamma \sim 4$–5. Thus, it seems that the IMBHs and their host star clusters do not lie on the extrapolation of the galactic scale SMBH scaling relations.

https://doi.org/10.1017/S1743921325104523 Published online by Cambridge University Press

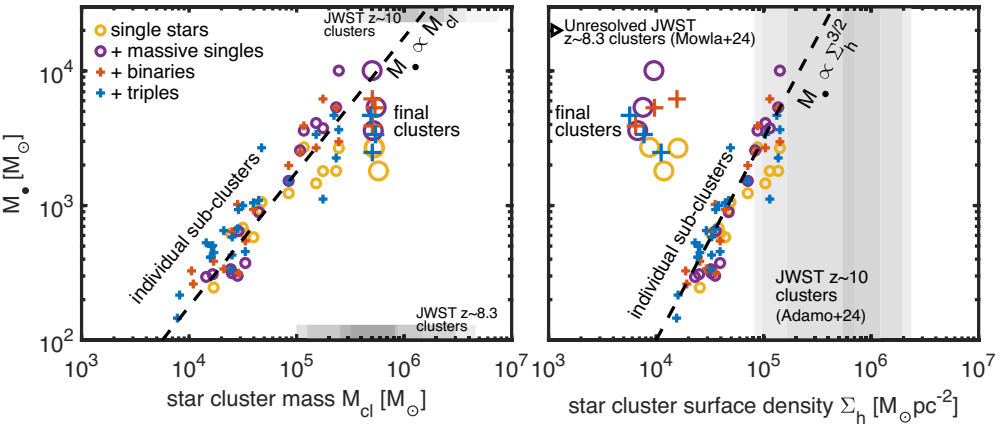


Figure 4. The scaling relations between the IMBH masses $M_\bullet$ and their host star cluster properties (Rantala *et al.* 2025). We distinguish between the initial sub-clusters (small symbols) and final assembled clusters (large symbols). Left panel: the correlation between the cluster mass $M_{\rm cl}$ and the IMBH masses. The individual sub-cluster masses show a clear correlation with their IMBH masses. Right panel: the case of the half-mass surface density $\Sigma_{\rm h}$. We find a tight correlation between $\Sigma_{\rm h}$ and the IMBH masses. Note that the final assembled cluster surface densities are well off the relation due to internal relaxation, stellar evolution and cluster mergers. Most interestingly, our results suggest the existence of IMBHs with masses exceeding $M_\bullet \gtrsim 10^4\,{\rm M}_\odot$ in the recent $z\sim10$ proto globular clusters observed with the JWST (Adamo *et al.* 2024).

The final assembled clusters are typically offset from the relations between the initial cluster properties and the IMBH masses. This is due to the evolution of the final assembling cluster. In the case of the cluster mass, the cluster assembly increases the mass of the central cluster by a factor of 4–5 while the most massive IMBH inherited from the sub-clusters can typically grow by a factor of up to ~2 via TDEs and BH mergers. Thus, the cluster grows more in stellar mass compared to IMBH mass growth and the final clusters end up in an offset from the $M_{\rm cl}$-$M_\bullet$ relation. The picture repeats for the velocity dispersion σ and especially the cluster half-mass surface density $\Sigma_{\rm h}$. Besides the mass growth, the assembling central cluster grows in half mass size due to internal relaxation effects, stellar evolution mass losses and star cluster mergers. This results in a larger offset of the final clusters from the $\Sigma_{\rm h}$–$M_\bullet$ and the σ–$M_\bullet$ relations compared to the scaling relation with mass.

Most interestingly, our scaling relations between the star cluster properties and the IMBH masses can be used to predict the IMBH masses in dense high redshift proto globular clusters observed by the JWST. While the Firefly Sparkle clusters (Mowla *et al.* 2024) at $z\sim8$ remain unresolved in size, we can nevertheless use our $M_{\rm cl}$–$M_\bullet$ relation to infer the cluster IMBH masses by assuming that the unresolved clusters are in reality denser than $\Sigma_{\rm h}\geq10^4$–$10^5\,{\rm M}_\odot\,{\rm pc}^{-2}$. This assumption yields $10^3\,{\rm M}_\odot\lesssim M_\bullet\lesssim10^4\,{\rm M}_\odot$ for the Firefly Sparkle clusters. For the resolved Cosmic Gems Arc clusters at $z\sim10$ (Adamo *et al.* 2024) we can use both the $M_{\rm cl}$–$M_\bullet$ and $\Sigma_{\rm h}$–$M_\bullet$ relations and predict IMBH masses in excess of $M_\bullet\gtrsim10^4\,{\rm M}_\odot$ for these proto globular clusters.

4. The characteristic gravitational wave fingerprint of hierarchical cluster assembly

We show in the Fig. 5 both the (IM)BH binaries in the hierarchical simulations at $t=10$ Myr as well as all the (IM)BH binaries that merged at any point before $t\leq10$ Myr. For comparison to the primary and secondary masses of the (IM)BH binaries we show the GW

https://doi.org/10.1017/S1743921325104523 Published online by Cambridge University Press

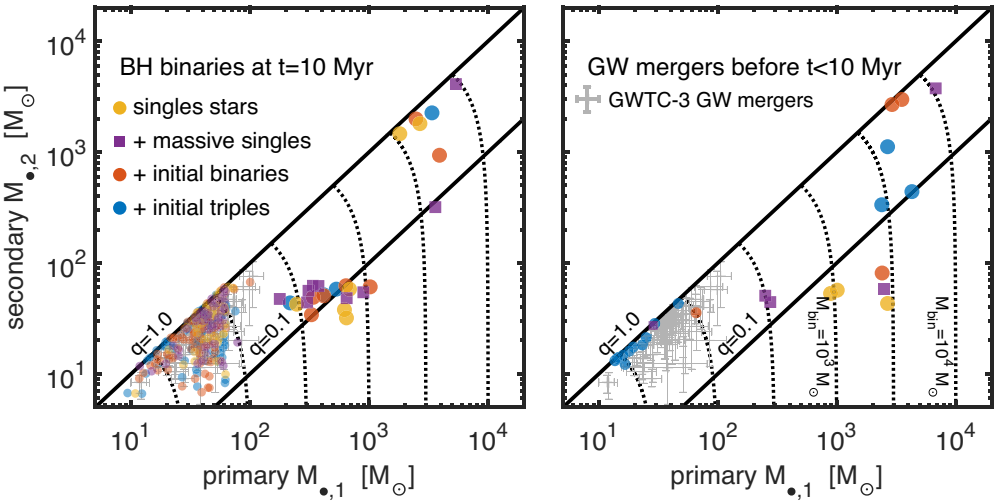


Figure 5. Left panel: the (IM)BH binaries and their primary and secondary BH masses in the final assembled clusters (Rantala and Naab 2025) at $t = 10$ Myr (filled circles and squares). The background crosses show the GW mergers in the LIGO-Virgo-KAGRA GWTC-3 catalogue (Abbott *et al.* 2023). Our stellar BH binary population coincides with the LVK mass range very well. Besides the stellar binaries, the simulations at $t = 10$ Myr contain IMBH-BH binaries with primary masses $300\,\mathrm{M}_\odot \lesssim M_\bullet \lesssim 10^3\,\mathrm{M}_\odot$ and mass ratios close to $q \sim 0.1$. Finally IMBH-IMBH binaries with total masses up to $M_\bullet \sim 10^4\,\mathrm{M}_\odot$ and close to equal mass ratios $q \sim 1$ form in the models. Right panel: the GW driven BH-BH, IMBH-BH and IMBH-IMBH mergers before $t = 10$ Myr. The rapid close to equal mass ratio IMBH-IMBH merger is the characteristic GW fingerprint of the hierarchical star cluster assembly scenario.

observations from the GWTC-3 catalogue (Abbott *et al.* 2023) detected by the Advanced LIGO and Advanced Virgo GW observatories up to the end of their third observing run. Our results represent high redshift mergers which would be unobservable with current GW instruments. Still, the fact that both our stellar BH-BH binaries and stellar BH-BH GW mergers coincide the GWTC-3 parameter space acts as a straightforward validation of our initial conditions and our stellar evolution approach.

For stellar BH binaries and mergers the monolithic isolated cluster formation model and the hierarchical assembly scenario are expected to produce very similar results. On the contrary, for especially IMBH-IMBH mergers a considerably different picture emerges. As one dense isolated star cluster typically only forms a single IMBH, the assembly history of a massive star cluster strongly affects its gravitational wave output. In the hierarchical assembly scenario IMBH-IMBH binaries can frequently form, harden and rapidly merge within only 10 Myr, often driven by triple IMBH interactions. In the monolithic cluster formation scenario such complex interactions would be exceedingly rare. In Fig. 5, we show the populations of IMBH-BH and IMBH-IMBH binaries and GW mergers in our hierarchical simulations. The IMBH-BH binaries have primary masses of $300\,\mathrm{M}_\odot \lesssim M_\bullet \lesssim 10^3\,\mathrm{M}_\odot$ and mass ratios close to $q \sim 0.1$ while the IMBH-BH mergers typically have larger primaries and accordingly smaller mass ratios. Both the IMBH-IMBH binaries and GW mergers occupy a parameter space of $3 \times 10^3\,\mathrm{M}_\odot \lesssim M_{\bullet,1} + M_{\bullet,2} \lesssim 10^4\,\mathrm{M}_\odot$ and $0.1 \lesssim q \lesssim 1.0$. We conclude that such rapid close to equal mass GW mergers in the IMBH mass range are the characteristic GW fingerprint of the hierarchical star cluster assembly model. The $z \gtrsim 10$ sensitivity for LISA rapidly increases between $M_\bullet \sim 10^3\,\mathrm{M}_\odot$ and $M_\bullet \sim 10^4\,\mathrm{M}_\odot$ (Amaro-Seoane *et al.* 2012). Thus, only our most massive GW mergers would most probably be observable by LISA at $z \gtrsim 10$ with signal-to-noise ratio SNR~ 10. However, our scaling relations in section 3 readily predict GW mergers observable by LISA in

https://doi.org/10.1017/S1743921325104523 Published online by Cambridge University Press

massive (nuclear) star clusters with $M_{\rm cl} > 10^6\,{\rm M}_\odot$. Our lower-mass IMBHs still remain targets for future space-based GW detector such as DECIGO (Kawamura *et al.* 2021) or TianQuin (Luo *et al.* 2016). Third-generation ground-based GW observatories such as the Einstein Telescope and the Cosmic Explorer will be sensitive to IMBH mergers with total masses of $M_{\rm bin} = M_{\bullet,1} + M_{\bullet,2} \lesssim 10^3\,{\rm M}_\odot$ at $z < 10$ (Reali *et al.* 2024; Abac *et al.* 2025).

5. Conclusions

We have studied the effect star cluster assembly and stellar multiplicity on the formation of extremely massive stars and IMBHs through runaway stellar collisions. We find that both the hierarchical assembly and stellar multiplicity boost the numbers and masses of IMBHs in the final assembled clusters. Moreover, the well motivated hierarchical cluster assembly scenario predicts a characteristic GW signature of close to equal mass GW mergers in the IMBH mass regime. Such mergers are considerably rare in our isolated comparison models. The rapid GW driven IMBH-IMBH mergers naturally connect the extreme high redshift star formation to IMBH and SMBH seed formation and the emerging field of high redshift GW astronomy.

In the future, we plan to extend our models to somewhat more metal enriched clusters (towards $Z \sim 0.1\,{\rm Z}_\odot$) as many high redshift proto galaxies and especially AGN are already metal enriched. Another intriguing opportunity are models including both accurate small scales stellar and BH dynamics as well as hydrodynamics. Such setups have become very recently feasible (Fujii *et al.* 2024; Lahén *et al.* 2025) thanks to the advances in modelling small-scale gravitational dynamics in larger-scale high resolution simulations (Rantala *et al.* 2017, 2020; Mannerkoski *et al.* 2023; Wang *et al.* 2020a).

References

Aarseth, S. J. 2003, Cambridge University Press.
Abac, A., Abramo, R., Albanesi, S., & et al. 2025, *arXiv e-prints*, arXiv:2503.12263.
Abbott, R., Abbott, T. D., Acernese, F., & et al. 2023, *Physical Review X*, 13(4), 041039.
Adamo, A., Bradley, L. D., Vanzella, E., & et al. 2024, 632(8025), 513–516.
Amaro-Seoane, P., Aoudia, S., Babak, S., & et al. 2012, *Classical and Quantum Gravity*, 29(12), 124016.
Amaro-Seoane, P., Konstantinidis, S., Dewi Freitag, M., & et al. 2014, *ApJ*, 782(2), 97.
Arca Sedda, M., Kamlah, A. W. H., Spurzem, R., & et al. 2024, *MNRAS*, 528(3), 5119–5139.
Bastian, N., Gieles, M., Efremov, Y. N., & Lamers, H. J. G. L. M. 2005, *A&A*, 443(1), 79–90.
Belokurov, V. & Kravtsov, A. 2022, *MNRAS*, 514(1), 689–714.
Brown, G. & Gnedin, O. Y. 2021, *MNRAS*, 508(4), 5935–5953.
Bunker, A. J., Saxena, A., Cameron, A. J., & et al. 2023, *A&A*, 677, A88.
Chin, S. A. 1997, *Physics Letters A*, 226(6), 344 – 348.
Cournoyer-Cloutier, C., Tran, A., Lewis, S., & et al. 2021, *MNRAS*, 501(3), 4464–4478.
Dehnen, W. & Hernandez, D. M. 2017, *MNRAS*, 465(1), 1201–1217.
Elmegreen, B. G. & Efremov, Y. N. 1996, *ApJ*, 466, 802.
Fahrion, K. & De Marchi, G. 2024, *A&A*, 681, A20.
Ferrarese, L. & Merritt, D. 2000, *ApJ*, 539(1), L9–L12.
Fregeau, J. M., Cheung, P., Portegies Zwart, S. F., & Rasio, F. A. 2004, *MNRAS*, 352(1), 1–19.
Fujii, M. S. & Portegies Zwart, S. 2013, *MNRAS*, 430(2), 1018–1029.
Fujii, M. S., Wang, L., Tanikawa, A., Hirai, Y., & Saitoh, T. R. 2024, *Science*, 384(6703), 1488–1492.
Fujimoto, S., Ouchi, M., Kohno, K., & et al. 2024, *arXiv e-prints*, arXiv:2402.18543.
Gaburov, E., Gualandris, A., & Portegies Zwart, S. 2008, *MNRAS*, 384(1), 376–385.
Gebhardt, K., Bender, R., Bower, G., & et al. 2000, *ApJ*, 539(1), L13–L16.
Glebbeek, E., Gaburov, E., de Mink, S. E., Pols, O. R., & Portegies Zwart, S. F. 2009, *A&A*, 497(1), 255–264.

https://doi.org/10.1017/S1743921325104523 Published online by Cambridge University Press

González Prieto, E., Weatherford, N. C., Fragione, G., Kremer, K., & Rasio, F. A. 2024, *ApJ*, 969(1), 29.
Greene, J. E., Strader, J., & Ho, L. C. 2020, *ARA&A*, 58, 257–312.
Gürkan, M. A., Freitag, M., & Rasio, F. A. 2004, *ApJ*, 604(2), 632–652.
Häring, N. & Rix, H.-W. 2004, *ApJ*, 604(2), L89–L92.
Inayoshi, K., Visbal, E., & Haiman, Z. 2020, *ARA&A*, 58, 27–97.
Iorio, G., Mapelli, M., Costa, G., & et al. 2023, *MNRAS*, 524(1), 426–470.
Isobe, Y., Maiolino, R., D'Eugenio, F., & et al. 2025, *arXiv e-prints*, arXiv:2502.12091.
Kawamura, S., Ando, M., Seto, N., & et al. 2021, *PTEP*, 2021(5), 05A105.
Kormendy, J. & Ho, L. C. 2013, *ARA&A*, 51(1), 511–653.
Kroupa, P. 2001, *MNRAS*, 322(2), 231–246.
Lahén, N., Naab, T., Johansson, P. H., & et al. 2020, *ApJ*, 891(1), 2.
Lahén, N., Naab, T., Rantala, A., & Partmann, C. 2025, *arXiv e-prints*, arXiv:2504.18620.
Luo, J., Chen, L.-S., Duan, H.-Z., & et al. 2016, *Classical and Quantum Gravity*, 33(3), 035010.
Maiolino, R., Scholtz, J., Curtis-Lake, E., & et al. 2024a, *A&A*, 691a, A145.
Maiolino, R., Scholtz, J., Witstok, J., & et al. 2024b, *Nature*, 627b(8002), 59–63.
Makino, J. & Aarseth, S. J. 1992, *PASJ*, 44, 141–151.
Mannerkoski, M., Rawlings, A., Johansson, P. H., & et al. 2023, *MNRAS*, 524(3), 4062–4082.
Mapelli, M. 2016, *MNRAS*, 459(4), 3432–3446.
Mapelli, M., Spera, M., Montanari, E., & et al. 2020, *ApJ*, 888(2), 76.
Marks, M. & Kroupa, P. 2012, *A&A*, 543, A8.
Meena, B., Sabbi, E., Zeidler, P., & et al. 2025, *arXiv e-prints*, arXiv:2505.02890.
Mezcua, M. 2017, *International Journal of Modern Physics D*, 26(11), 1730021.
Mikkola, S. & Tanikawa, K. 1999, *MNRAS*, 310(3), 745–749.
Moe, M. & Di Stefano, R. 2017, *ApJS*, 230(2), 15.
Mowla, L., Iyer, K., Asada, Y., & et al. 2024, *Nature*, 636(8042), 332–336.
Offner, S. S. R., Moe, M., Kratter, K. M., & et al. 2023, volume 534 of *ASOP Conference Series*, 275.
Plummer, H. C. 1911, *MNRAS*, 71, 460–470.
Portegies Zwart, S. F., Baumgardt, H., Hut, P., Makino, J., & McMillan, S. L. W. 2004, *Nature*, 428(6984).
Rantala, A., Lahén, N., Naab, T., Escobar, G. J., & Iorio, G. 2025, *arXiv e-prints*, arXiv:2506.04330.
Rantala, A. & Naab, T. 2025, *MNRAS*, 542(1), L78–L84.
Rantala, A., Naab, T., & Lahén, N. 2024, *MNRAS*, 531(3), 3770–3799.
Rantala, A., Naab, T., Rizzuto, F. P., & et al. 2023, *MNRAS*, 522(4), 5180–5203.
Rantala, A., Naab, T., & Springel, V. 2021, *MNRAS*, 502(4), 5546–5562.
Rantala, A., Pihajoki, P., Johansson, P. H., Naab, T., Lahén, N., & Sawala, T. 2017, *ApJ*, 840, 53.
Rantala, A., Pihajoki, P., Mannerkoski, M., Johansson, P. H., & Naab, T. 2020, *MNRAS*, 492(3), 4131–4148.
Reali, L., Cotesta, R., Antonelli, A., Kritos, K., Strokov, V., & Berti, E. 2024, *Phys. Rev. D*, 110(10), 103002.
Rees, M. J. 1984, *ARA&A*, 22, 471–506.
Reines, A. E. & Volonteri, M. 2015, *ApJ*, 813(2), 82.
Rizzuto, F. P., Naab, T., Rantala, A., & et al. 2023, *MNRAS*, 521(2), 2930–2948.
Rizzuto, F. P., Naab, T., Spurzem, R., & et al. 2021, *MNRAS*, 501(4), 5257–5273.
Sabbi, E., Sirianni, M., Nota, A., & Tosi, M. e. a. 2007, *AJ*, 133(1), 44–57.
Shepherd, K. G., Costa, G., & Ugolini, C. e. a. 2025, *arXiv e-prints*, arXiv:2505.10206.
Spera, M., Mapelli, M., & Bressan, A. 2015, *MNRAS*, 451(4), 4086–4103.
Spurzem, R. 1999, *Journal of Computational and Applied Mathematics*, 109, 407–432.
Topping, M. W., Stark, D. P., Senchyna, P., & et al. 2024, *MNRAS*, 529(4), 3301–3322.
Übler, H., Maiolino, R., Pérez-González, P. G., & et al. 2024, *MNRAS*, 531(1), 355–365.
Vergara, M. C., Askar, A., & Flammini Dotti, F. e. a. 2025,a *arXiv e-prints*, arXiv:2508.14260.

https://doi.org/10.1017/S1743921325104523 Published online by Cambridge University Press

Vergara, M. C., Askar, A., Kamlah, A. W. H., & et al. 2025,b *arXiv e-prints*, arXiv:2505.07491.
Wang, L., Iwasawa, M., Nitadori, K., & Makino, J. 2020,a *MNRAS*, 497a(1), 536–555.
Wang, L., Nitadori, K., & Makino, J. 2020,b *MNRAS*, 493b(3), 3398–3411.
Whitmore, B. C., Chandar, R., Schweizer, F., & et al. 2010, *AJ*, 140(1), 75–109.
Winters, J. G., Henry, T. J., Jao, W.-C., & et al. 2019, *AJ*, 157(6), 216.
Yan, Z., Jerabkova, T., & Kroupa, P. 2023, *A&A*, 670, A151.
Zlochower, Y. & Lousto, C. O. 2015, *Phys. Rev. D*, 92(2), 024022.

https://doi.org/10.1017/S1743921325104523 Published online by Cambridge University Press